35th Annual International Conference of the IEEE EMBS
Osaka, Japan, 3 - 7 July, 2013

A Novel Through-Wall Respiration Detection Algorithm Using UWB Radar

Xin Li, Dengyu Qiao, Ye Li* and Huhe Dai

Abstract— **Through-wall respiration detection using Ultra-wideband (UWB) impulse radar can be applied to the post-disaster rescue, e.g., searching living persons trapped in ruined buildings after an earthquake. Since strong interference signals always exist in the real-life scenarios, such as static clutter, noise, etc., while the respiratory signal is very weak, the signal to noise and clutter ratio (SNCR) is quite low. Therefore, through-wall respiration detection using UWB impulse radar under low SNCR is a challenging work in the research field of searching survivors after disaster. In this paper, an improved UWB respiratory signal model is built up based on an even power of cosine function for the first time. This model is used to reveal the harmonic structure of respiratory signal, based on which a novel high-performance respiration detection algorithm is proposed. This novel algorithm is assessed by experimental verification and simulation and shows about a 1.5dB improvement of SNR and SNCR.**

I. Introduction

Non-contact through-wall life detection using UWB impulse radar is helpful for searching survivors in the debris after disaster. In fact, UWB impulse radar endowed with high range resolution and high penetrability offers an attractive technique to search trapped people hidden by obstacles by detecting their respiration. In [1-5], feasibility studies on detecting respiration using UWB radar have been conducted in recent years. Additionally, some other studies [6-7] address human respiration detection under low SNCR and aim to design a high-performance threshold-based detection algorithm. In [6], singular value decomposition (SVD) in frequency domain and constant false alarm threshold are used to decide the existence and position of human beings. In [7], the trapped victim signature is identified in the range-frequency matrix by using method based on constant false alarm ratio (CFAR) and clustering. In these previous works, most of efforts are spent to detect the fundamental harmonic and researchers neglect high order harmonics existing in the periodic respiratory signal. Therefore, a new detection algorithm specialized in detecting periodical signal containing multiple harmonics is more suitable for the respiration detection than those previous works focusing on the fundamental harmonic of respiratory signal.

In this paper, an improved UWB respiratory signal model is firstly built up based on an even power of a cosine function, which reveals the harmonic structure of respiratory signal. Then, a novel threshold-based detection algorithm is proposed based on the harmogram defined by Hinich [8], who provides a powerful detection approach based on the prior knowledge of the harmonic structure of periodic signal. This novel algorithm will exhibit a better performance in comparison with the previous work [7], since it detects the respiratory signal by its harmonic structure.

This paper is organized as follows. In section II, the UWB respiratory signal model and the system model of real-life echo matrix are demonstrated. The novel detection algorithm is proposed in Section III. Section IV presents the experimental result and performance analysis.

II. UWB Respiratory Signal Model and System Model

A. UWB Respiratory Signal Model

Breathing motion can be approximated by an absolute value [9] or an even power [10] of a cosine function. Considering the scenario that one person is facing a radar sensor, the radial distance between the chest surface of the inspected person and the radar can be modeled as follows:

$$d(t) = d_0 - B \times (\cos \pi f_r t)^u , \quad (1)$$

where d_0 is the distance of the inspected person, B is the amplitude of the chest surface radial motion, normally between 5mm and 15mm [11], f_r is the respiratory frequency, normally between 0.2Hz and 0.5Hz, and u is the power of cosine function which must be even. Fig. 1 shows an example of $d(t)$ whose parameter settings are given in TABLE I. Impulse radar signals are usually sampled in time and there are

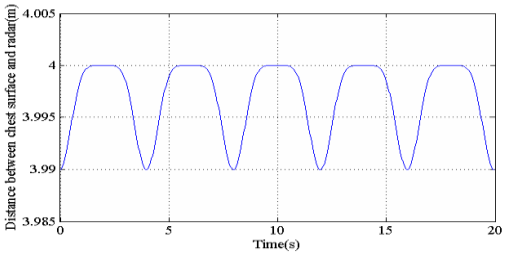

Figure 1. Distance between chest surface and radar. Parameter setting is given in TABLE I.

TABLE I. Parameter Settings for Echo Matrix Simulation

Parameter	Value	Parameter	Value
u	6	A	10^{-9}
d_0	4m	ρ	128ps
B	10mm	T_{st}	0.05s
f_r	0.25Hz	T_{ft}	50ps

Research is supported in part by the National Science Foundation of China (NO.31000447), Key Lab for Health Informatics of Chinese Academy of Science(NO.CXB201104220026A) and Basic Research Program of Shenzhen (NO.JC201005270258A).

Xin Li (e-mail: xin.li@siat.ac.cn), Dengyu Qiao (e-mail: dy.qiao@siat.ac.cn), Ye Li* (corresponding author, e-mail: ye.li@siat.ac.cn), Huhe Dai are with the Shenzhen Institutes of Advanced Technology, Chinese Academy of Sciences, Key Lab for Health Informatics of Chinese Academy of Science.

two time axes, i.e., fast-time and slow-time [12]. Assuming one pulse is transmitted at slow-time t, the time delay of the round-trip travel from the antenna to the chest surface

$$t_d(t) = 2 \times d(t)/c \,, \tag{2}$$

where c is the speed of light. Next, let's focus on the fast-time domain and denote the radar impulse by $p(s)$, where s is the fast-time variable. If a pulse sent at t is reflected by the chest surface, the reflection signal

$$r^t(s) = p\left(s - t_d(t)\right). \tag{3}$$

The impulse generated by the radar used in this paper can be approximated by 1st order Gaussian function

$$p(s) = -A \times \frac{2s}{\rho^2} \times e^{-\frac{s^2}{\rho^2}}, \tag{4}$$

where A is the amplitude factor and ρ is the time factor. If substituting (1), (2) and (4) into (3) and considering $r^t(s)$ as a function of both t and s, we get

$$r(t,s) = -A \times \frac{2 \times \left(s - \frac{2 \times \left(d_0 - B\left(\cos \pi f_r t\right)^u\right)}{c}\right)}{\rho^2} \times e^{-\frac{\left(s - \frac{2 \times \left(d_0 - B\left(\cos \pi f_r t\right)^u\right)}{c}\right)^2}{\rho^2}}. \tag{5}$$

Then, the discrete time respiratory echo matrix can be expressed as follows:

$$r[m,n] = r\left(mT_{st}, nT_{ft}\right), \tag{6}$$

where m and T_{st} are the discrete time variable and the sampling interval in the slow-time domain, respectively, and n and T_{ft} are the discrete time variable and the sampling interval in the fast-time domain, respectively. Fig. 2, shows a simulated echo matrix $r[m,n]$. In this paper, a denotation rule is made for convenience, that is for any signal matrix $\Re[m,n]$, $\Re^m[n]$ is used to represent the mth fast-time signal in the echo matrix, which is just the mth row vector of $\Re$, and similarly $\Re^n[m]$ is used to represent the nth slow-time signal, which is just the nth column vector of $\Re$. $r_{DC}^n[m]$, the DC component of $r^n[m]$, will be removed by clutter suppression algorithm. We denote the harmonic component of $r^n[m]$ by $r_h^n[m]$ where

$$r_h^n[m] = r^n[m] - r_{DC}^n[m]. \tag{7}$$

Fig. 3 shows a Discrete Fourier Transform (DFT) matrix whose column vector is the DFT of $r_h^n[m]$ which is extracted from the echo matrix shown in Fig. 2, and according to the harmonic structure shown in Fig. 3, the power of the first two harmonics is dominant in the total power of $r_h^n[m]$.

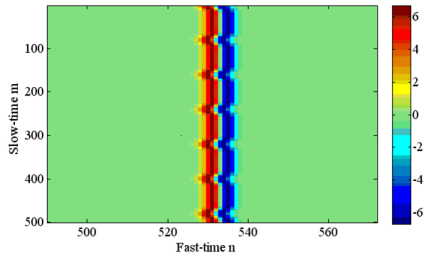

Figure 2. Simulated echo matrix. Parameter setting is given in TABLE I.

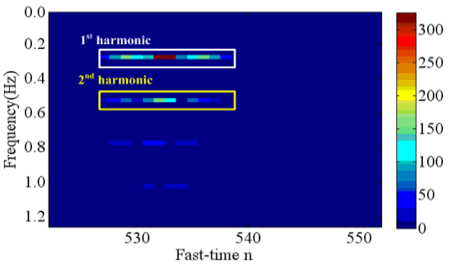

Figure 3. DFT matrix of $r_h^n[m]$ which is extracted from the echo matrix shown in Fig. 2

B. System Model of Real-life Echo Matrix

In the real-life scenario of detecting a person by UWB impulse radar, the raw echo matrix

$$R[m,n] = r[m,n] + c[n] + w[m,n] + d[m] + l[m,n], \tag{8}$$

where $r[m,n]$ is the respiratory echo, $c[n]$ is the background static clutter, $w[m,n]$ denotes the additive white Gaussian noise (AWGN), $d[m]$ denotes the unstable fast-time DC component, and $l[m,n]$ denotes the slow-time linear trend, which results from the amplitude instability of the data acquisition equipment.

III. Detection Algorithm

The detection algorithm is divided into three stages: filtering in the fast-time domain, linear trend and static clutter suppression, and threshold-based detection.

A. Filtering in the fast-time domain

Due to the amplitude instability of the radar system, an unstable fast-time DC component $d[m]$ will be introduced into the echo matrix. In order to remove $d[m]$, a band-pass fast-time linear phase FIR filter, whose pass-band match the band of the radar impulse, is applied to process the echo matrix. The filter output matrix $R_{ftF}[m,n]$ is expressed by (9), where $h_{ftF}[n]$ denotes the filter impulse response, $*_n$ denotes the signal convolution in the fast-time domain, δ_{ftF} is the filter group delay, w_{ftF} is the filter output of $w[m,n]$, and l_{ftF} is the filter output of $l[m,n]$. Since $w[m,n]$ is an AWGN, it is easy to find that $w_{ftF}^n[m]$ is still an AWGN in the slow-time domain.

$$\begin{aligned} R_{ftF}^m[n] &= R^m[n] *_n h_{ftF}[n] \\ &= r^m[n] *_n h_{ftF}[n] + c[n] *_n h_{ftF}[n] + w^m[n] *_n h_{ftF}[n] + d[m] *_n h_{ftF}[n] + l^m[n] *_n h_{ftF}[n] \\ &= r^m\left[n - \delta_{ftF}\right] + c\left[n - \delta_{ftF}\right] + w_{ftF}^m[n] + l_{ftF}^m[n] \end{aligned} \tag{9}$$

B. Linear trend and static clutter suppression

The linear trend subtraction (LTS) algorithm is based on estimating the slow-time DC component and any potential slow-time linear trend existing in echo matrix by means of a linear least-square fit [13]. Supposing the size of signal matrix $R_{ftF}[m,n]$ is $M \times N$, the estimate of the DC component of $R^n_{ftF}[m]$ is subsequently subtracted from itself, resulting in:

$$R^n_{LTS}[m] = R^n_{ftF}[m] - x\left(x^T x\right)^{-1} x^T R^n_{ftF}[m], \quad (10)$$

where $x = \left[\aleph / M \quad 1_M\right]$, $\aleph = [0\ 1\ \ldots\ M\text{-}1]^T$, and 1_M is an $M \times 1$ vector containing unit values. By the LTS algorithm, $r_{DC}[m,n\text{-}\delta_{ftF}]$, $c[n\text{-}\delta_{ftF}]$ and $l_{ftF}[m,n]$ in $R_{ftF}[m,n]$ will be effectively removed. As a result, we get

$$R^n_{LTS}[m] = r_h^{n-\delta_{ftF}}[m] + w^n_{ftF}[m] - x\left(x^T x\right)^{-1} x^T w^n_{ftF}[m]. \quad (11)$$

As M is always very large, the 3rd term in the right side of (11), which is used to estimate the DC component of AWGN $w^n_{ftF}[m]$, will extremely approximate to a zero vector. Then,

$$R^n_{LTS}[m] = r_h^{n-\delta_{ftF}}[m] + w^n_{ftF}[m]. \quad (12)$$

C. Threshold-based detection

According to the harmogram defined by Hinich [8], we define the harmogram matrix

$$H(\omega, n) = \sum_{j=1}^{J}\left[I_n(\omega_j) / \hat{S}_n(\omega_j)\right], \quad (13)$$

where ω is the radian frequency, $\omega_j = \omega \times j$, I_n is the periodogram [14] of R^n_{LTS}, and $\hat{S}_n(\omega_j)$ is the estimate for the power spectrum of w^n_{ftF} at ω_j. According to the harmonic structure of the UWB respiratory signal, the first two harmonics hold the major signal power, so J=2. As w^n_{ftF} is a white noise, its power spectrum is constant, i.e., $S_n(\omega)=\sigma_n^2$, where σ_n^2 is the value of the noise power. Therefore, if we get an estimate of σ_n^2, denoted by $\hat{\sigma}_n^2$, then (13) can be reformulated as

$$H(\omega, n) = \sum_{j=1}^{J}\left[I_n(\omega_j) / \hat{\sigma}_n^2\right] = \left[\sum_{j=1}^{J} I_n(\omega_j)\right] / \hat{\sigma}_n^2. \quad (14)$$

If FFT algorithm is applied to compute periodogram, $I_n(\omega)$ will be computed for a finite number of radian frequency values as follows:

$$I_n(\omega_k) = \left|X^n_{LTS}[k]\right|^2 / M, \ k=0,1,2,\ldots,M\text{-}1, \quad (15)$$

where $\omega_k = 2\pi k / M$ and $X^n_{LTS}[k]$ is the DFT of $R^n_{LTS}[m]$. An approach to estimate σ_n^2 based on $I_n(\omega_k)$ is given as follows:

$$\hat{\sigma}_n^2 = \left[\sum_{\underline{\omega} \le \omega_k \le \bar{\omega}} I_n(\omega_k)\right] / K, \quad (16)$$

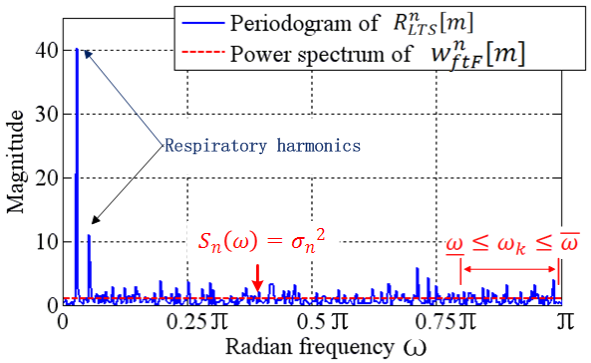

Figure 4. Periodogram of $R^n_{LTS}[m]$ and power spectrum of $w^n_{ftF}[m]$

where K is the number of ω_k between radian frequency $\underline{\omega}$ and $\bar{\omega}$, and the choice of values of $\underline{\omega}$ and $\bar{\omega}$ should make sure that in the radian frequency band from $\underline{\omega}$ to $\bar{\omega}$ there only exists noise. Fig. 4 shows an example of how to use (16) to estimate σ_n^2. As the respiratory harmonics only appear in the low frequency band, the high frequency band can be used to estimate σ_n^2, and the setting that $\underline{\omega} = 0.8\pi$ and $\bar{\omega} = \pi$ obviously satisfies the corresponding requirement.

Hypothesis testing on whether a respiratory signal exists or not is performed on the harmogram:

$$H(\omega, n) \underset{H_0}{\overset{H_1}{\gtrless}} \gamma, \quad (17)$$

where H_1 denotes the hypothesis that there exists a respiratory signal, and H_0 denotes the null hypothesis. The threshold γ should be properly set to make this detector keep an acceptable false alarm rate.

IV. Experimental Result and Performance Analysis

A. Experimental Result

The measurement system consists of a UWB radar sensor and a laptop for data storing and processing. The UWB impulse radar sends a 1st–order derivative Gaussian pulse whose -10dB bandwidth is 0.45~3.555GHz. Fig. 5 shows the sketch of the laboratory setup. During the observation, the person keeps breathing without any other movement. The experimental result is shown in Fig. 6. The respiratory signal can be visually inspected in the output matrix of the LTS algorithm and successfully detected by a threshold-based decision on the harmogram matrix.

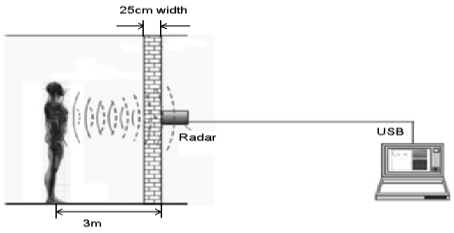

Figure 5. The sketch of the laboratory setup for experiment

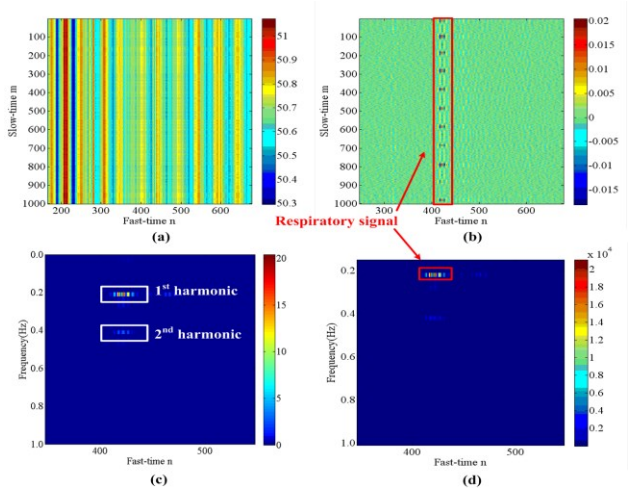

Figure 6. Experimental result: (a) raw echo matrix $R[m,n]$; (b) output matrix after LTS algorithm, $R_{LTS}[m,n]$; (c) Periodogram matrix $I(\omega,n)$; (d) Harmogram matrix $H(\omega,n)$.

B. Performance Analysis

In the performance analysis against SNR and SNCR, the simulated signal shown in Fig. 2 is regarded as the target respiratory signal. One thousand clutter samples with proper size are acquired by the experimental system when there are no people breathing behind the wall. Figs. 7 and 8 show the detection performance of the proposed algorithm and the reference algorithm [7]. SNR and SNCR are defined by (18), where P_r denotes the power of the respiratory signal, P_w denotes noise power, P_c denotes clutter power, T_r is the respiratory period, and $M' \times N'$ is the size of the data matrix $R_{fiF}[m,n]$, which is the fast-time filter output matrix of clutter sample. Finally, the analysis result shows that the proposed algorithm has about a 1.5dB improvement of SNR and SNCR in comparison with the reference algorithm [7].

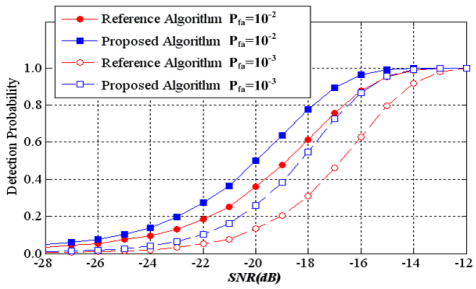

Figure 7. Detection probability as a function of SNR*

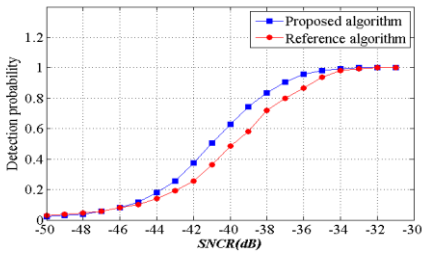

Figure 8. Detection probability as a function of SNCR*, P_{fa}=0.01

* Key parameter setting for simulation: M=1200, J=2, T_{st}=0.05s, T_{fi}=50ps, $\underline{\omega} = 0.8\pi$, $\overline{\omega} = \pi$, M'=1200, N'=120; for the reference algorithm [7], I_x=1, G_x=3, O_x=5, I_y=9, G_y=13, O_y=17.

$$SNR = P_r / P_w,\ SNCR = P_r / P_c,$$
$$P_r = \sum_{m=1}^{T_r/T_{st}} \sum_{n=527}^{538} r[m,n]^2 \Big/ 12T_r/T_{st}, \qquad (18)$$
$$P_c = \sum_{m=0}^{M'-1} \sum_{n=0}^{N'-1} \left(R_{fiF}[m,n]\right)^2 \Big/ M' \times N'$$

V. Conclusion

In this paper, an improved UWB respiratory echo model is built up to reveal the harmonic structure of respiratory signal, based on which a novel respiration detection algorithm using UWB impulse radar is designed. By performance analysis, we show that this novel algorithm has about a 1.5dB improvement of SNR and SNCR in comparison with the previous work [7].

References

[1] J. Sachs, M. Aftanas, S. Crabbe, M. Drutarovsky, R. Klukas, D. Kocur, *et al.*, "Detection and Tracking of Moving or Trapped People Hidden by Obstacles using Ultra-Wideband Pseudo-Noise Radar," *2008 European Radar Conference,* pp. 408-411, 2008.

[2] G. Ossberger, T. Buchegger, E. Schimback, A. Stelzer, and R. Weigel, "Non-Invasive Respiratory Movement Detection and Monitoring of Hidden Humans Using Ultra Wideband Pulse Radar," *Joint Uwbst & Iwuwbs 2004, Conference Proceedings,* pp. 395-399, 2004.

[3] I. Y. Immoreev, "Practical Application of Ultra-Wideband Radars," *Ultrawideband and Ultrashort Impulse Signals, Proceedings,* pp. 44-49, 2006.

[4] Q. Wang, Y. Li, J. Wu, and T. Y. Zhang, "Life Signal Extraction in Through-the-Wall Surveillance," *Embc: 2009 Annual International Conference of the IEEE Engineering in Medicine and Biology Society, Vols 1-20,* pp. 1343-1346, 2009.

[5] M. Baboli, O. Boric-Lubecke, and V. Lubecke, "A New Algorithm for Detection of Heart and Respiration Rate with UWB Signals," *Engineering in Medicine and Biology Society (EMBC), 2012,* pp. 3947-3950, 2012.

[6] A. Nezirovic, A. G. Yarovoy, and L. P. Ligthart, "Signal Processing for Improved Detection of Trapped Victims Using UWB Radar," *IEEE Transactions on Geoscience and Remote Sensing,* vol. 48, pp. 2005-2014, Apr 2010.

[7] Y. Y. Xu, S. Y. Wu, C. Chen, J. Chen, and G. Y. Fang, "A Novel Method for Automatic Detection of Trapped Victims by Ultrawideband Radar," *IEEE Transactions on Geoscience and Remote Sensing,* vol. 50, pp. 3132-3142, Aug 2012.

[8] M. J. Hinich, "Detecting a Hidden Periodic Signal When Its Period Is Unknown," *IEEE Transactions on Acoustics Speech and Signal Processing,* vol. 30, pp. 747-750, 1982.

[9] A. Nezirovic, A. G. Yarovoy, and L. P. Ligthart, "Experimental Study on Human Being Detection Using UWB Radar," *Radar Symposium, 2006. IRS 2006. International,* pp. 1-4, 2006.

[10] Y. Seppenwoolde, H. Shirato, K. Kitamura, S. Shimizu, M. van Herk, J. V. Lebesque, *et al.*, "Precise and Real-Time Measurement of 3D Tumor Motion in Lung Due to Breathing and Heartbeat, Measured During Radiotherapy," *International Journal of Radiation Oncology Biology Physics,* vol. 53, pp. 822-834, Jul 15 2002.

[11] L. B. Liu, Z. J. Liu, and B. E. Barrowes, "Through-Wall Bio-Radiolocation With UWB Impulse Radar: Observation, Simulation and Signal Extraction," *IEEE Journal of Selected Topics in Applied Earth Observations and Remote Sensing,* vol. 4, pp. 791-798, Dec 2011.

[12] M. Soumekh, *Fourier Array Imaging*. Englewood Cliffs, New Jersey: Prentice-Hall, Inc., 1994.

[13] A. Nezirovic, "Stationary Clutter- and Linear-trend Suppression in Impulse-Radar-based Respiratory Motion Detection," *2011 IEEE International Conference on Ultra-Wideband (ICUWB),* pp. 331-335, 2011.

[14] A. V. Oppenheim, R. W. Schafer, and J. R. Buck, *Discrete-Time Signal Processing, 2nd ed*. Upper Saddle River, NJ: Prentice-Hall, 1999.